

SHORT COMMUNICATION

Chiral resolution, determination of absolute configuration, and biological evaluation of (1,2-benzothiazin-4-yl)acetic acid enantiomers as aldose reductase inhibitors

Xin Hao, Xiangyu Qin, Saghir Hussain, Shagufta Parveen, Wei Zhang, Fengyan Fu, Bing Ma, and Changjin Zhu

Department of Applied Chemistry, Beijing Institute of Technology, Beijing, China

Abstract

A novel series of (1,2-benzothiazin-4-yl)acetic acid enantiomers was prepared by chiral resolution, and their absolute configurations were determined using the PGME method. The biological evaluation of the racemate and single enantiomers has shown a remarkable difference for the aldose reductase inhibitory activity and selectivity. The (R)-(–)-enantiomer exhibited the strongest aldose reductase activity with an IC_{50} value of 0.120 μ M, which was 35 times more active than the S-(+)-enantiomer. Thus, the stereocenter at the C4 position of this scaffold was shown to have a major impact on the activity and selectivity.

Keywords

Absolute configuration determination, aldose reductase inhibitors, 1,2-benzothiazine 1,1-dioxide, chiral resolution

History

Received 3 August 2014
Accepted 31 August 2014
Published online 27 November 2014

Introduction

Diabetes mellitus (DM) is a common metabolic disease caused by a deficiency in production of insulin or by insulin resistance in cells. Hyperglycemia accompanying the disease is the primary cause of long-term diabetic complications, such as neuropathy, retinopathy, nephropathy and atherosclerosis, because a significant portion of glucose is forced to enter into the polyol pathway^{1–3}. Growing evidence reveals that diabetic complications are related to an increased activity of the enzyme aldose reductase (ALR2, EC 1.1.1.21) in the pathway^{4,5}. ALR2 is the first enzyme of this metabolic pathway to catalyze the NADPH-dependent reduction of glucose to sorbitol^{2,6}. Thus, inhibition of ALR2 represents an attractive approach to prevent or delay the progression of diabetic complications. Various ALR2 inhibitors (ARIs) have been reported but only epalrestat has been marketed so far⁷, and many ARIs have been renounced either for their undesirable effects or insufficient efficacy. Hence, development of more ARIs is needed.

In our effort to design and synthesize new ARIs, we have found a series of (1,1-dioxido-1,2-benzothiazin-4-yl) substituted acetic acid derivatives (Figure 1) having good ALR2 inhibitory activity⁸. Particularly, this class has a chiral carbon atom C4 to which the acetate head, the key anion group for binding to ALR2, is attached. The chirality of C4 provides a good handle not only to study the structure–activity relationships (SAR) with regard to the configuration of the anion head but also to gain further insight into the structural profile of the active site of the enzyme. However, until now this series of compounds is available in

racemic form only, and the absolute configuration at the chiral center of the single enantiomers remains to be established.

The interest in synthesizing biologically active products containing stereogenic carbon atoms has notably increased over the last decade, and chirality is currently of major importance in drug discovery and development⁹. With the development of new technologies, the preparation of enantiomerically pure compounds is frequently requested because of the different activities of drug enantiomers in pharmaceutical applications^{10–12}. Consequently, current requirements from legal regulation have largely increased the number of enantiomerically pure drugs rather than racemates presented for approval¹³. As one class of classic ARIs, spirohydantoin including sorbinil¹⁴, fidarestat¹⁵ and ranirestat¹⁶, which also contain a stereogenic center, were prepared in the enantiomerically pure forms as shown in Figure 1.

Therefore, as an extension of our previous work, we have engaged in preparing the enantiomerically pure acids. In the present study, the racemic 2-[2-(2,4,5-trifluorobenzyl)-1,1-dioxido-3,4-dihydro-2H-1,2-benzothiazin-4-yl]acetic acid ((±)-**1**) having the highest inhibitory activity in this series was chosen to resolve the corresponding enantiomers and to determine their absolute configuration and stereostructure–activity relationships.

Materials and methods

General

All reactions were routinely checked by TLC on silica gel Merck 60F₂₅₄. ¹H NMR spectra were recorded at 400 MHz, while ¹³C NMR spectra were recorded at 100 MHz. Chemical shifts are given in δ units (ppm) relative to internal standard TMS and refer to CDCl₃ solutions. MS was performed with a

Address for correspondence: Changjin Zhu, Department of Applied Chemistry, Beijing Institute of Technology, No. 5, Zhongguancun South Street, Beijing 100081, China. E-mail: zcj@bit.edu.cn

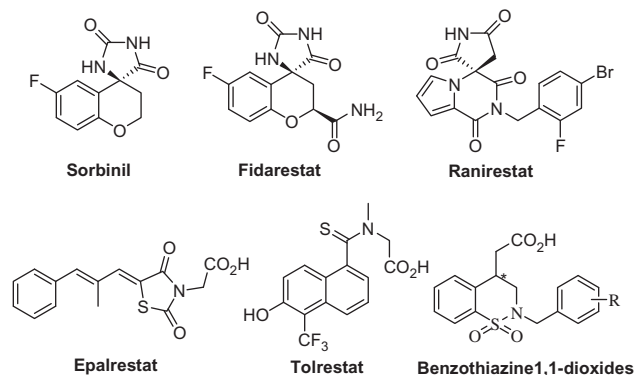


Figure 1. Chemical structures of aldose reductase inhibitors.

Varian 500-MS ion trap mass spectrometer equipped with an ESI source. Optical rotations were measured at the indicated concentration of g/100 mL. Melting points were recorded on an X-4 microscopic melting point apparatus and were uncorrected. Aldehyde reductase (ALR1, EC 1.1.1.2) and ALR2 were prepared according to the method of Kinoshita¹⁷ and Concettina La Motta¹⁸. Enzyme activity was assayed spectrophotometrically on a Shimadzu UV-1800 UV spectrophotometer by measuring the decrease in absorption of NADPH at $\lambda = 340$ nm.

Synthesis of racemic acid (\pm)-1

The racemic 2-[2-(2,4,5-trifluorobenzyl)-1,1-dioxido-3,4-dihydro-2H-1,2-benzothiazin-4-yl]acetic acid ((\pm) -**1**) was prepared according to the synthetic pathway reported previously⁸.

Synthesis of diastereomeric amides (+)-5 and (–)-5

To a solution of (\pm)-**1** (1 mmol) in DMF: chloroform (12 mL, 1:3) was added HOBT (1.5 mmol) and EDCI (2.5 mmol) in sequence. The reaction mixture was stirred at room temperature overnight. After the formation of the activated ester, L-(–)- α -methylbenzylamine (1 mmol) and Et₃N (0.3 mL) were added. The reaction was allowed to stir for 6 h and then water (15 mL) was added. The mixture was extracted with ethyl acetate (2 \times 15 mL), and the combined organic layers were washed with brine (10 mL), dried over MgSO₄, and concentrated in vacuo. Separation by column chromatography using ethyl acetate/petroleum ether (1:4) as the eluant afforded the title compounds (+)-**5** ($R_f = 0.26$, ethyl acetate/petroleum ether, 1:1) and (–)-**5** ($R_f = 0.29$, ethyl acetate/petroleum ether, 1:1).

Synthesis of the enantiomers (+)-1 and (–)-1

A solution of **5** (3 mmol) in dioxane (10 mL) was treated with 6 N HCl (8 mL) and refluxed for 10 h. The mixture was cooled, basified to pH 14 with NaOH 32% in water, diluted with water (25 mL) and extracted with dichloromethane (2 \times 30 mL). The resulting solution was acidified to pH 1 with 9 N HCl, extracted with dichloromethane (3 \times 30 mL). The combined organic layers were dried over MgSO₄ and evaporated in vacuum to give the desired compound. The crude product was purified by silica gel chromatography (CH₂Cl₂/CH₃OH; 100:1).

(+)-2-[2-(2,4,5-Trifluorobenzyl)-1,1-dioxido-3,4-dihydro-2H-1,2-benzothiazin-4-yl]acetic acid ((+)-**1**). Pale yellow powder (0.87 g, 75%); m.p.: 79–81 °C; $[\alpha]_D^{20} = +7.26$ (c 1.132, CH₂Cl₂); ¹H NMR (400 MHz, CDCl₃) δ : 7.90 (d, $J = 8.0$ Hz, 1H), 7.54 (t, $J = 7.6$ Hz, 1H), 7.46 (t, $J = 7.6$ Hz, 1H), 7.36–7.29 (m, 2H), 6.97–6.90 (m, 1H), 4.60 (d, $J = 14.8$ Hz, 1H), 4.15 (d, $J = 14.8$ Hz, 1H), 3.84 (dd, $J = 14.8, 4.8$ Hz, 1H), 3.65

(dd, $J = 14.4, 6.4$ Hz, 1H), 3.56–3.51 (m, 1H), 2.71–2.69 (m, 2H); ¹³C NMR (100 MHz, CDCl₃) δ : 175.94, 137.46, 136.85, 132.91, 128.61, 128.29, 124.77, 119.19, 118.99, 106.13, 105.93, 105.86, 105.65, 49.42, 43.50, 38.50, 32.31; MS m/z : negative mode 384.1 ([M–H][–]), positive mode 408.2 ([M+Na]⁺).

(–)-2-[2-(2,4,5-Trifluorobenzyl)-1,1-dioxido-3,4-dihydro-2H-1,2-benzothiazin-4-yl]acetic acid ((–)-**1**). Pale yellow powder (0.82 g, 71%); m.p.: 80–82 °C; $[\alpha]_D^{20} = -7.58$ (c 1.214, CH₂Cl₂); ¹H NMR (400 MHz, CDCl₃) δ : 7.90 (d, $J = 6.8$ Hz, 1H), 7.54 (t, $J = 6.4$ Hz, 1H), 7.46 (t, $J = 7.6$ Hz, 1H), 7.36–7.28 (m, 2H), 6.96–6.90 (m, 1H), 4.61 (d, $J = 14.4$ Hz, 1H), 4.14 (d, $J = 14.8$ Hz, 1H), 3.84 (dd, $J = 14.4, 4.8$ Hz, 1H), 3.63 (dd, $J = 14.0, 6.0$ Hz, 1H), 3.55–3.49 (m, 1H), 2.72–2.70 (m, 2H); ¹³C NMR (100 MHz, CDCl₃) δ : 176.53, 137.25, 136.74, 132.83, 128.49, 128.23, 124.67, 119.07, 118.93, 106.03, 105.82, 105.75, 105.54, 49.18, 43.32, 38.31, 32.24; MS m/z : negative mode 384.1 ([M–H][–]), positive mode 386.2 ([M+H]⁺), 408.3 ([M+Na]⁺).

Enzymatic assay

ALR1 activity was performed at 37 °C in a reaction mixture containing 0.12 mM NADPH (0.25 mL), enzyme extract (0.1 mL), 0.1 M sodium phosphate buffer (pH 7.2, 0.25 mL), deionized water (0.15 mL) and 20 mM sodium D-glucuronate (0.25 mL) as substrate in a final volume of 1 mL. The reaction mixture except for sodium D-glucuronate was incubated at 37 °C for 10 min. The substrate was then added to start the reaction, which was monitored for 4 min. ALR2 activity was performed at 30 °C in a reaction mixture containing 0.10 mM NADPH (0.25 mL), 0.1 M sodium phosphate buffer (pH 6.2, 0.25 mL), enzyme extract (0.1 mL), deionized water (0.15 mL) and 10 mM D,L-glyceraldehyde (0.25 mL) as substrate in a final volume of 1 mL. The reaction mixture except for D,L-glyceraldehyde was incubated at 30 °C for 10 min. The substrate was then added to start the reaction, which was monitored for 4 min.

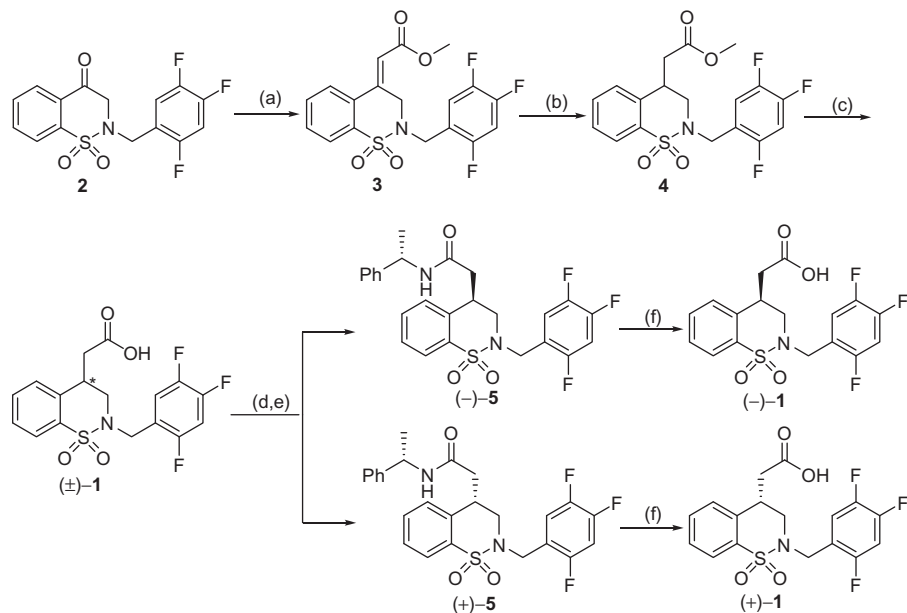
The inhibitory activity of the newly synthesized compounds against ALR2 and ALR1 was assayed by adding 5 μ L of the inhibitor solution to the reaction mixture described above. All compounds were dissolved in dimethyl sulfoxide (DMSO) and diluted with deionized water. To correct for the non-enzymatic oxidation of NADPH, the rate of NADPH oxidation in the presence of all of the reaction mixture components except the substrate was subtracted from each experimental rate. The inhibitory effect of the synthetic compounds was routinely estimated at a concentration of 10^{–5} M (the concentration is referred to that of the compound in the reaction mixture). Those compounds found to be active were tested at additional concentrations between 10^{–5} and 10^{–7} M. Each dose–effect curve was generated using at least three concentrations of inhibitor causing an inhibition between 20 and 80% with three replicates at each concentration.

Results and discussion

Synthetic chemistry

The racemic compound (\pm)-**1** was prepared according to the previously reported procedure depicted in Scheme 1⁸, starting with the preparation of the corresponding α,β -unsaturated ester as precursor of the targeted C4-enantiomers. Wittig olefination of the N-substituted ketone **2** with methyl 2-(triphenylphosphoranylidene) acetate provided α,β -unsaturated ester **3**¹⁹. Subsequent Pd/C-catalyzed hydrogenation gave the corresponding ester **4**²⁰, which was converted to racemic acid (\pm)-**1** by hydrolysis with aqueous sodium hydroxide. Our next goal was the chiral resolution of (\pm)-**1**. Efforts to resolve (\pm)-**1** by conversion

Scheme 1. Reagents and conditions:
 (a) $\text{Ph}_3\text{P}=\text{CHCOOCH}_3$, PhCH_3 , reflux;
 (b) H_2 , 10% Pd/C, MeOH, AcOEt;
 (c) 1,4-dioxane, NaOH; (d) HOBT,
 EDCl, CHCl_3 , DMF, room temperature;
 (e) L-(−)-α-methylbenzylamine, Et_3N ;
 (f) 1,4-dioxane, 6 N HCl, reflux.



to diastereomeric esters were unsuccessful due to poor chromatographic separation of the ester products. However, (±)-1 could be resolved by forming diastereomeric amides **5** with L-(−)-α-methylbenzylamine via reaction with the N-hydroxybenzotriazole activated ester intermediate. The two amides (+)-**5** and (−)-**5** were separated by column chromatography and in turn converted into the free acids (+)-**1** and (−)-**1**, respectively, by acid hydrolysis²¹. The acids (+)-**1** and (−)-**1** were analyzed for their enantiomeric purity using chiral HPLC: enantiomeric excesses were 95.2 and 97.9%, respectively. This result confirmed the successful preparation of the single enantiomers of compound **1**.

Determination of absolute configuration

Following isolation of the separated enantiomers, it was essential to determine the absolute configurations of (+)-**1** and (−)-**1**. ¹H-NMR analysis of diastereomeric derivatives is one of the few methods capable of establishing the absolute configuration of chiral compounds. Reaction with a chiral agent turns the enantiomers into diastereomeric derivatives, for which distinct chemical shift changes can be correlated to their absolute configurations. Phenylglycine methyl ester (PGME), a chiral anisotropic reagent, has been developed for the elucidation of the absolute configuration of chiral carboxylic acids by means of ¹H-NMR²², and the technique also proved to be successful in the present study.

The principle of the PGME method applied to (+)-**1** and (−)-**1** is outlined in Figure 2: a chiral β,β-disubstituted propionic acid is condensed with (R)- and (S)-PGME, respectively, giving the corresponding diastereomeric amides. In order for the PGME benzene ring to exert a predictable diamagnetic field effect upon R₁ or R₂, the backbone formed by the PGME amide and propionic carbon chain needs to occur in one plane. In the most stable conformation of the PGME amide of a β,β-disubstituted propionic acid, this plane is fixed by the presence of an amide linkage and dipole–dipole interaction between the methoxycarbonyl group and the amide carbonyl²². If the conformation shown at the bottom of Figure 2 is correct for the PGME amide of a β,β-disubstituted propionic acid, the protons H_{X-Z} would be more shielded by the benzene ring of the (R)-PGME moiety than those of the (S)-PGME amide. The reverse would be true for H_{A-C} which are more shielded in the (R)-PGME amide. Therefore, the

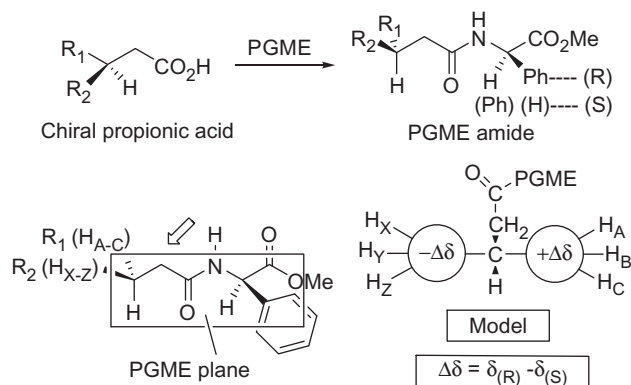


Figure 2. The principle of the PGME method.

absolute configuration at the β-position of the chiral propionic acid can be determined using the model $[\Delta\delta = \delta_{(R)} - \delta_{(S)}]$ in Figure 2. According to this principle, the ¹H-NMR shift differences $\Delta\delta$ between the diastereomeric (R)- and (S)-PGME amides arising from the enantiomers (+)-**1** and (−)-**1** were calculated, respectively, and the results are shown in Figure 3. Without exception, the negative $\Delta\delta$ values were on the same side of the molecule as the PGME benzene ring in (+)-**6** and (−)-**6**, and the positive $\Delta\delta$ values were on the opposite side. These results allowed assignments of the S absolute configuration to (+)-**1** and the R one to (−)-**1**. Thus, the PGME method has been successfully applied to determine the absolute configurations of (+)-**1** and (−)-**1**.

Aldose reductase inhibition and SAR studies

The single enantiomers were then tested for their potential inhibitory effect on ALR2 isolated from rat lenses. The IC₅₀ values were determined by linear regression analysis of the log of the concentration–response curve⁸. The results of these biological evaluations are listed in Table 1, and the effectiveness of the test compounds was evaluated with respect to the potent ALR2 inhibitor epalrestat used as a positive control. Compounds (rac)-(±)-**1**, (R)-(−)-**1** and (S)-(+)-**1** all showed significant

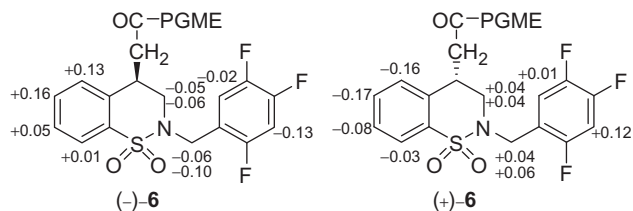


Figure 3. $\Delta\delta$ values obtained for the PGME amides (–)-**6** and (+)-**6**.

inhibitory activity against ALR2. Of these isomers, (R)-(–)-**1** was found to be the most active having an IC_{50} value of 0.120 μ M comparable to that of epalrestat (Table 1). In contrast, (S)-(+)-**1** was less effective with an IC_{50} value of 4.174 μ M. Here, for the first time, we have demonstrated that the (R)- and (S)-enantiomers of 1,2-benzothiazine-1,1-dioxide-based acetic acid ARIs inhibit aldose reductase to a largely different extent and specified the (R)-(–)-enantiomer as the stronger ARI.

In order to evaluate the selectivity of the ALR2 inhibition, the isomers were also tested for the inhibition against ALR1 isolated from rat kidney. The enzyme ALR1 is most closely related to ALR2²³ and plays a detoxification role^{24,25}. Many failures of ARIs in clinic trial stages are believed to be mainly due to a lack of selectivity²⁶. Clearly, the isomer (R)-(–)-**1** having the most potent activity in the ALR2 inhibition showed a significantly lower activity in the ALR1 inhibition compared with other isomers (Table 1), indicating an excellent selectivity for (R)-(–)-**1**.

Therefore, our results suggest that the orientation of the acetic acid head at the C4 position of this class not only plays a key role for the binding with ALR2 but also has an important function in discriminating and excluding homologous enzymes. Actually, there is often a large difference in biological activity between the enantiomers of chiral drugs¹¹.

Molecular modeling

Docking studies were performed in an attempt to investigate the difference in ALR2 inhibitory activity between the enantiomers and propose a binding mode that explains the above-described SARs. (R)-**1** and (S)-**1** were individually docked into the conformation of human ALR2 from the complex with NADP⁺/IDD594 (PDB code: 1US0) as shown in Figure 4.

Analysis of the docking results revealed that the carboxylic acid head of (R)-**1** formed three tight hydrogen bonds with the OH of Tyr48 (2.73 Å), the N ϵ 2 atom of His110 (2.83 Å) and the N ϵ 1 of Trp111 (2.90 Å), respectively, imbedded deeply into the anion binding pocket of the enzyme. Further, the benzyl ring was deeply trapped in the hydrophobic cage of the specificity pocket and in turn π -stacked perfectly against the indole moiety of Trp111. These interactions anchored (R)-**1** tightly within the enzyme active site. In the docking of (S)-**1**, it was found that one oxygen atom of the sulfur dioxide group formed only one hydrogen bond with Trp111 (3.51 Å), while the carboxylic acid head showed no binding interaction with the active site of the enzyme. Though the carboxylic acid side chain residue was oriented away from the anion binding pocket, the benzyl ring showed π -stacking with Trp111 and was well placed into the specificity pocket. The docking results suggested different binding modes for (R)-**1** and (S)-**1**, which extended their differently oriented C4-carboxylic acid heads into different positions of the active site. The carboxylic acid side chain of (R)-**1** showed a favorable binding interaction with the anion pocket of the enzyme ALR2,

Table 1. Biological activity data for 1,2-benzothiazine 1,1-dioxide acetic acid derivatives.

Compound	ALR2 IC_{50} * (μ M)	ALR1 (% of inhibition) [†]
(rac)-(\pm)- 1	0.676 (0.589–0.763)	14.7
(R)-(–)- 1	0.120 (0.084–0.156)	7.5
(S)-(+)- 1	4.174 (3.692–4.656)	11.8
Epalrestat	0.086 (0.059–0.112)	73.6

* IC_{50} (95% CL) values represent the concentration required to produce 50% enzyme inhibition.

[†]The inhibitory effect was estimated at a concentration of 10 μ M.

while its benzyl group pointed into the deep direction of the specificity pocket. This may explain the higher inhibitory activity of (R)-**1** compared to that of (S)-**1**, providing the basis for our surmise in the SAR studies.

Conclusion

The two key amines were employed throughout the chemistry in the present study. First, racemic acid (\pm)-**1** was coupled with L-(–)- α -methylbenzylamine to produce diastereomeric amides, which resulted in the chiral resolution of the 1,2-benzothiazine-1,1-dioxide based racemic ARIs with excellent enantiomeric purities. Then, the separated single enantiomers (–)-**1** and (+)-**1** were coupled again with both of the enantiomeric (R)- and (S)-phenylglycine methyl esters used as chiral anisotropic reagents, to yield four diastereomeric amides; NMR analysis of these coupling products enabled the assignment of the absolute configurations (R)-(–)-**1** and (S)-(+)-**1** to the enantiomers. These results allowed to study the stereostructure–activity relationships and selectivity in the ALR2 inhibition, and to gain insight into the mechanism of binding of the key carboxylate head group with the active site of ALR2.

Biological investigations of the single enantiomers showed that (R)-(–)-**1** was approximately 35 times more active than (S)-(+)-**1** and also had much better selectivity in the ALR2 inhibition. In agreement with the biological results, docking studies indicated a more favored interaction for binding of (R)-(–)-**1** with the active site of the enzyme than that for binding of (S)-(+)-**1**. Consequently, the stereogenic C4 position of these 1,2-benzothiazine-1,1-dioxide-based ARIs has a major impact on both the activity and selectivity of the ALR2 inhibition; hence, chirality could be considered as a useful tool in the lead optimization process, at least in the case of this class of ARIs (Supplementary material).

Declaration of interest

The authors report no conflicts of interest. This work was supported by the National Natural Science Foundation of China (grant no. 21272025), the Research Fund for the Doctoral Program of Higher Education of China (grant no. 20111101110042), the Science and Technology Commission of Beijing, China (grant no. Z131100004013003) and the Beijing Natural Science Foundation (grant no. 3100021501401).

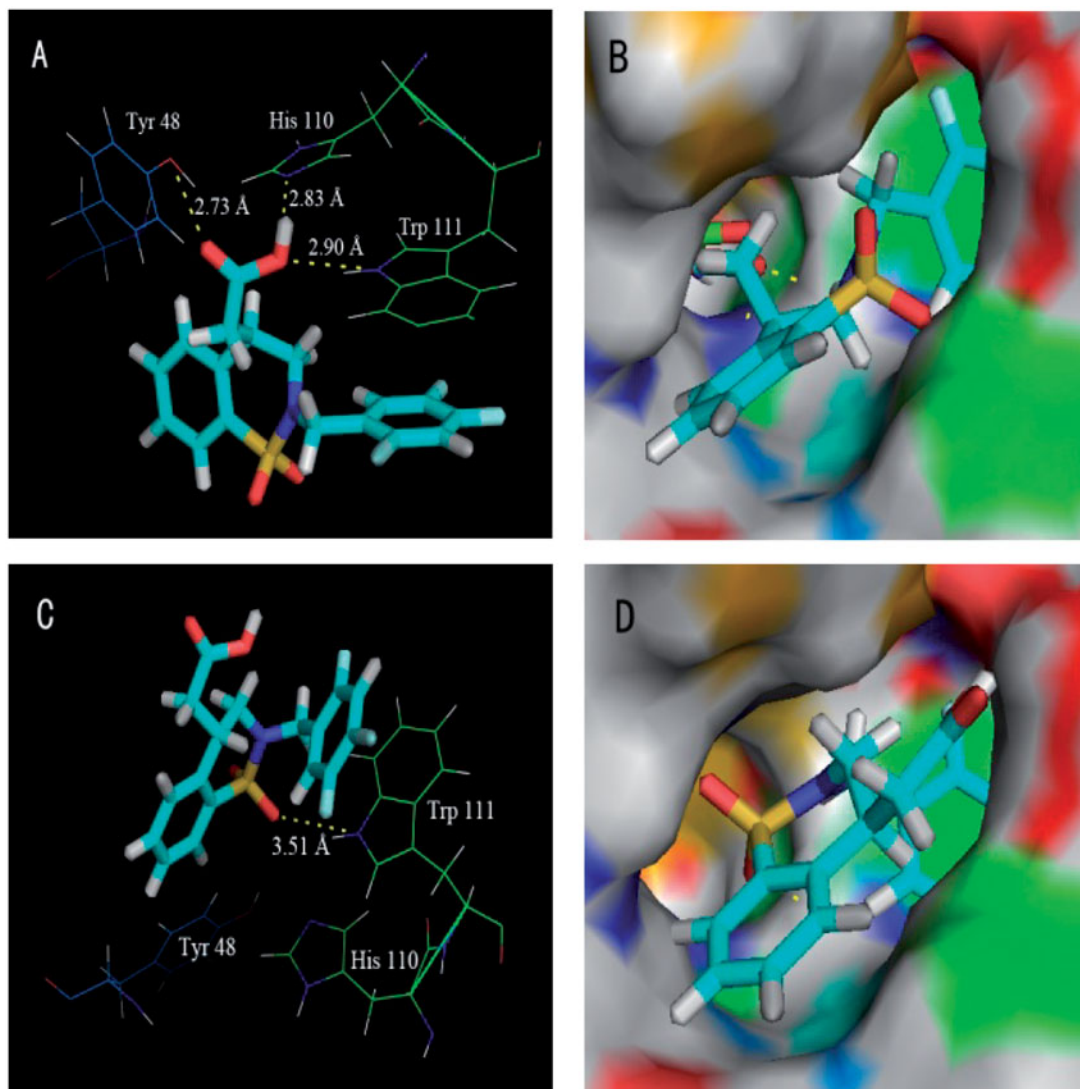


Figure 4. Molecular docking of inhibitors (R)-1 and (S)-1 into the active site of ALR2. A and B presents docking for (R)-1, while C and D for (S)-1, respectively. Ligands are shown as stick models, while the selected and labeled protein residues are presented (A and C) in line representation and (B and D) in surface representation. Docked poses of compounds are shown in cyan (C), red (O), blue (N), yellow (S) and gray (F); hydrogen bonds are shown as yellow dashed lines.

References

- Van Heyningen R. Formation of polyols by the lens of the rat with 'Sugar' cataract. *Nature* 1959;184:194–5.
- Gabbay KH, Merola LO, Field RA. Sorbitol pathway: presence in nerve and cord with substrate accumulation in diabetes. *Science* 1966;151:209–10.
- Chung SSM, Chung SK. Genetic analysis of aldose reductase in diabetic complications. *Curr Med Chem* 2003;10:1375–87.
- Moczulski DK, Burak W, Doria A, et al. The role of aldose reductase gene in the susceptibility to diabetic nephropathy in Type II (non-insulin-dependent) diabetes mellitus. *Diabetologia* 1999;42:94–7.
- Kao YL, Donaghue K, Chan A, et al. A novel polymorphism in the aldose reductase gene promoter region is strongly associated with diabetic retinopathy in adolescents with type 1 diabetes. *Diabetes* 1999;48:1338–40.
- Kinoshita JH, Nishimura C. The involvement of aldose reductase in diabetic complications. *Diabetes Metab Rev* 1988;4:323–37.
- Ramirez MA, Borja NL. Epalrestat: an aldose reductase inhibitor for the treatment of diabetic neuropathy. *Pharmacotherapy* 2008;28:646–55.
- Chen X, Zhang SZ, Yang YC, et al. 1,2-Benzothiazine 1,1-dioxide carboxylate derivatives as novel potent inhibitors of aldose reductase. *Bioorgan Med Chem* 2011;19:7262–9.
- Fuji K. Asymmetric creation of quaternary carbon centers. *Chem Rev* 1993;93:2037–66.
- Mentel M, Blankenfeldt W, Breinbauer R. The active site of an enzyme can host both enantiomers of a racemic ligand simultaneously. *Angew Chem Int Ed* 2009;48:9084–7.
- Kasprzyk-Hordern B. Pharmacologically active compounds in the environment and their chirality. *Chem Soc Rev* 2010;39:4466–503.
- Carey JS, Laffan D, Thomson C, Williams MT. Analysis of the reactions used for the preparation of drug candidate molecules. *Org Biomol Chem* 2006;4:2337–47.
- Beck G. Synthesis of chiral drug substances. *Synlett* 2002;2002:837–50.
- Costantino L, Rastelli G, Vianello P, et al. Diabetes complications and their potential prevention: Aldose reductase inhibition and other approaches. *Med Res Rev* 1999;19:3–23.
- Asano T, Saito Y, Kawakami M, et al. Fidarestat (SNK-860), a potent aldose reductase inhibitor, normalizes the elevated sorbitol accumulation in erythrocytes of diabetic patients. *J Diabetes Complicat* 2002;16:133–8.
- Negoro T, Murata P, Ueda S, et al. Novel, highly potent aldose reductase inhibitors: (R)-(-)-2-(4-bromo-2-fluorobenzyl)-1,2,3,4-tetrahydropyrrolo[1,2- α]pyrazine-4-spiro-3'-pyrrolidine-1,2',3,5'-tetrone (AS-3201) and its congeners. *J Med Chem* 1998;41:4118–29.

17. Hayman S, Kinoshita JH. Isolation and properties of lens aldose reductase. *J Biol Chem* 1965;240:877-82.
18. La Motta C, Sartini S, Mugnaini L, et al. Pyrido[1,2-a]pyrimidin-4-one derivatives as a novel class of selective aldose reductase inhibitors exhibiting antioxidant activity. *J Med Chem* 2007;50:4917-27.
19. Vine WH, Hsieh K-H, Marshall GR. Synthesis of fluorine-containing peptides. Analogs of angiotensin II containing hexafluorovaline. *J Med Chem* 1981;24:1043-7.
20. Da Settimo F, Primofiore G, Da Settimo A, et al. Novel, highly potent aldose reductase inhibitors: cyano (2-oxo-2,3-dihydroindol-3-yl) acetic acid derivatives. *J Med Chem* 2003;46:1419-28.
21. Kurono M, Kondo Y, Yamaguchi T, et al. Hydantoin derivatives for treating complications of diabetes. Google Patents; 1989.
22. Yabuuchi T, Kusumi T. Phenylglycine methyl ester, a useful tool for absolute configuration determination of various chiral carboxylic acids. *J Org Chem* 2000;65:397-404.
23. El-Kabbani O, Wilson DK, Petrash M, Quioco FA. Structural features of the aldose reductase and aldehyde reductase inhibitor-binding sites. *Mol Vis* 1998;4:19.
24. Ratliff DM, VanderJagt DJ, Eaton RP, VanderJagt DL. Increased levels of methylglyoxal-metabolizing enzymes in mononuclear and polymorphonuclear cells from insulin-dependent diabetic patients with diabetic complications: aldose reductase, glyoxalase I, and glyoxalase II - a clinical research center study. *J Clin Endocr Metab* 1996;81:488-92.
25. Carper DA, Wistow G, Nishimura C, et al. A superfamily of nadp-dependent reductases in eukaryotes and prokaryotes. *Exp Eye Res* 1989;49:377-88.
26. Sturm K, Levstik L, Demopoulos VJ, Kristl A. Permeability characteristics of novel aldose reductase inhibitors using rat jejunum in vitro. *Eur J Pharm Sci* 2006;28:128-33.

Supplementary material available online